JACS
JOURNAL OF THE AMERICAN CHEMICAL SOCIETY

Article

pubs.acs.org/JACS

Toward an Understanding of Diamond sp^2-Defects with Unsaturated Diamondoid Oligomer Models

Tatyana S. Zhuk,[⊥] Tatyana Koso,[‡] Alexander E. Pashenko,[⊥] Ngo Trung Hoc,[⊥] Vladimir N. Rodionov,[⊥] Michael Serafin,[§] Peter R. Schreiner,*[,‡] and Andrey A. Fokin*[,⊥,‡]

[⊥]Department of Organic Chemistry, Kiev Polytechnic Institute, pr. Pobedy 37, 03056 Kiev, Ukraine

[‡]Institute of Organic Chemistry, Justus-Liebig University, Heinrich-Buff-Ring 58, 35392 Giessen, Germany

[§]Institute of Inorganic Chemistry, Justus-Liebig University, Heinrich-Buff-Ring 58, 35392 Giessen, Germany

Supporting Information

ABSTRACT: Nanometer-sized doubly bonded diamondoid dimers and trimers, which may be viewed as models of diamond with surface sp^2-defects, were prepared from corresponding ketones via a McMurry coupling and were characterized by spectroscopic and crystallographic methods. The neutral hydrocarbons and their radical cations were studied utilizing density functional theory (DFT) and ab initio (MP2) methods, which reproduce the experimental geometries and ionization potentials well. The van der Waals complexes of the oligomers with their radical cations that are models for the self-assembly of diamondoids, form highly delocalized and symmetric electron-deficient structures. This implies a rather high degree of σ-delocalization within the hydrocarbons, not too dissimilar to delocalized π-systems. As a consequence, sp^2-defects are thus also expected to be nonlocal, thereby leading to the observed high surface charge mobilities of diamond-like materials. In order to be able to use the diamondoid oligomers for subsequent surface attachment and modification, their C—H-bond functionalizations were studied, and these provided halogen and hydroxy derivatives with conservation of unsaturation.

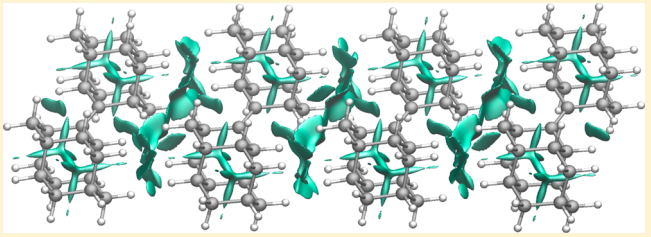

INTRODUCTION

Diamond-based materials are of great value for nanotechnology[1,2] due to unique combinations of strength, hardness,[3] semiconductivity when doped,[4] negative electron affinity (NEA) resulting in monochromatic electron emission,[5] ultraviolet photoluminescence,[6,7] and shape-dependent optical absorption.[8,9] Unlike other diamond-based materials, physically and chemically well characterized nanometer-sized diamondoids[8] (nanodiamonds) have well-defined sizes and shapes.[9] These are key requirements for carbon materials as building blocks in nanoscale electronic devices.[10,11] Recently, we realized an all-hydrocarbon molecular rectifier by linking the sp^3 (diamondoid) and sp^2 (fullerene) carbon allotropes.[12] Self-assembled monolayers (SAMs) of functionalized diamondoids on Au, Ag,[13] and metal oxide[14] surfaces display theoretically predicted[15] monochromatic electron emission with up to 70% electron yield for [121]tetramantane (**1**) derivatives.[16] Notably, the size of the diamondoid is decisive, as only low intensity emission was found for diamantane derivatives.[17,18] These properties are related to quantum confinement (QC) effects: for instance, the ionization potential (IP) of adamantane (9.24 eV) drops to 8.20 eV for **1** (Figure 1).[15] Further studies, however, are hampered because pure diamondoids larger than hexamantane are only available in mg quantities or even less; not even NMR data are available for these higher diamondoids.[19,20] The preparation of tailor-made larger diamondoid structures is possible through multiple sp^3−sp^3 or sp^2−sp^2 CC bond couplings of smaller diamondoids; 1-adamantyl-1-adamantane (**2**) and 2-(2-adamantylidene)adamantane (**3**)[21] are the simplest known representatives.[22]

While the sp^3−sp^3 diamondoid dimers reproduce parts of the hydrogen-terminated diamond lattice, dimer **3** is a model for the presence of sp^2-defects in diamond (Figure 1). The inclusion of unsaturation in diamondoids is a promising route for tuning the electronic properties of diamond-based materials, as we recently[23] demonstrated that the occupied states of the sp^2-dimers[24] are highly delocalized. The latter also determines the size-dependent properties, such as conductivity or electron emission. As the unsaturated bridge increases the electron conductivity as shown in molecular junction measurements, we hope that such oligomers will not only model the electronic properties of diamond with sp^2-defects, but also shed light on the nature of QC effects in large diamond nanoparticles. For instance, it was demonstrated that **3** already forms[25] a long-lived highly delocalized ionized species.[26] Additionally, the presence of unsaturation lowers the diamondoid oligomers' excitation energies relative to pristine diamondoids.[24] The construction of diamond-like materials based on **3** and its higher homologues is possible by their self-assembly on metal

Received: February 16, 2015
Published: April 27, 2015

DOI: 10.1021/jacs.5b01555
J. Am. Chem. Soc. 2015, 137, 6577−6586

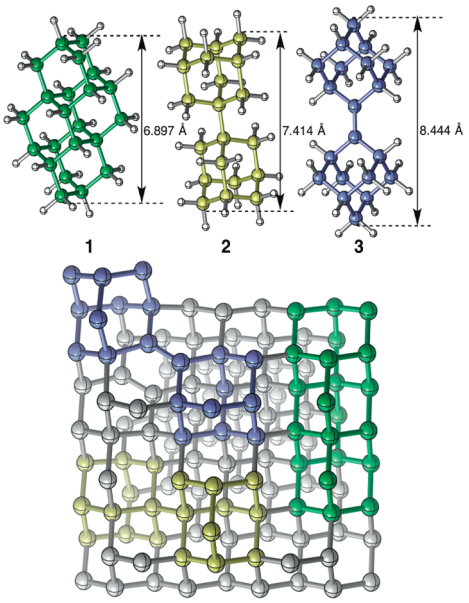

Figure 1. Structures and dimensions of [121]tetramantane (**1**), 1-adamantyl-1-adamantane (**2**), and 2-(2-adamantylidene)adamantane (**3**), and their representation as a part of the diamond lattice.

surfaces, as we have shown previously for the corresponding saturated derivatives.[27] The SAMs constructed from **3** are expected to display distinctly different properties due to the presence of sp^2-defects. As the intermolecular noncovalent forces are responsible for SAM formation,[28] we also compare our findings with appropriately chosen van der Waals clusters. Herein, we present the preparation and structural analysis of nanometer-sized diamondoid oligomers containing C=C bonds. This sheds light on the properties of large unsaturated hydrocarbon systems and aids in developing new diamond materials.

RESULTS AND DISCUSSION

Preparation and Structural Characterization of Diamondoid Oligomers.[29] The simplest sp^2-coupled diamondoid **3** was prepared through McMurry coupling[30,31] of adamantanone (**4**). This method gives better yields than the heterocondensation of **4** with hydrazine and H_2S followed by oxidative extrusion of sulfur with $Pb(OAc)_4$.[32] Diamondoid ketones of various sizes and topologies (Scheme 1) are readily available from direct oxidation of the respective diamondoids with sulfuric acid.[29] Diamantane-3,10-dione (**7**), a building block for double-couplings, was prepared via the reaction of 3-diamantanone (**5**) with 100% nitric acid, subsequent hydrolysis of the intermediate nitroxy derivative and oxidation of thus obtained mixture of hydroxy ketones with 99% sulfuric acid (Scheme 1). Diketone **7** was isolated as the main reaction product together with diamantane-3,8-dione (**10**). Diamondoid ketones **4**–**6** as well as **7** readily undergo McMurry coupling to give the corresponding diamondoid dimers, namely **3**, *syn*-3-(3-diamantylidene)diamantane (**11**), *anti*-3-(3-diamantylidene)-diamantane (**12**), 3-(2-adamantylidene)diamantane (**13**), 8-(2-adamantylidene)triamantane (**14**), 8-(8-triamantylidene)-triamantane (**15**) as well as 3,10-bis-(2-adamantylidene)-diamantane (**16**) (Table 1). The reactions were carried out

Scheme 1. Structures of Adamantane-2-one (4), Diamantane-3-one (5), triamantane-8-one (6), Diamantane-3,10-dione (7), and the Two-Step Oxidation of 5 to Diketones 7 and 10

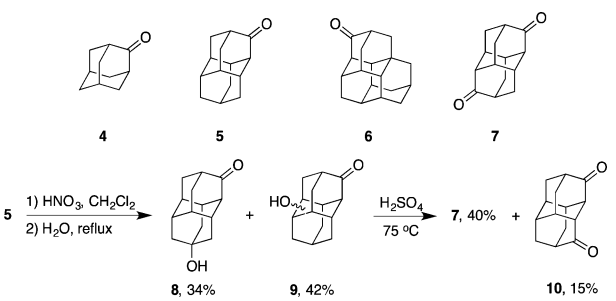

Table 1. Coupling of Ketones 4–7 and Preparative Yields of Diamondoid Dimers 3, 11–16

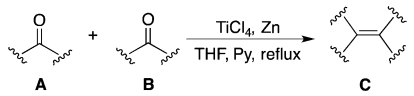

#	Starting ketone A	Starting ketone B	Products, C
1	 **4**	4	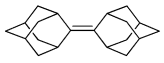 **3**, 42%
2	 **5**	5	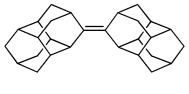 **11**, 37% 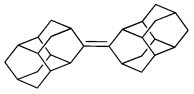 **12**, 37%
3	4	5	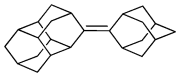 **13**, 47% **3**, 9% **11**, 16% **12**, 18%
4	 **6**	4	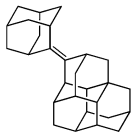 **14**, 51% 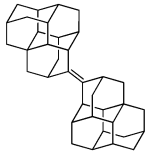 **15**, 15%
5	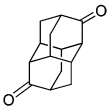 **7**	4	 **16**, 87%

under inert atmosphere by adding the ketone to the reagent prepared from titanium tetrachloride and zinc powder under reflux in dry tetrahydrofuran.[33] The isolation and purification of the products required several crystallizations (see Experimental for details). All dimers were fully characterized and all NMR resonances were assigned through a comparative analysis of COSY, HSQC, and HMBC-TOCSY spectra as well X-ray crystal structure analysis (see Supporting Information, SI).

From the X-ray crystal structure analysis we found that dimers **3**, **11**–**13** display C=C bonds lengths (1.325–1.335 Å, Figure 2) that are close to the standard value of 1.34 Å.[34] In analogy to parent **3** where the hydrogen locations are based on the "neutronographic" values of 1.1 Å along the electron-

DOI: 10.1021/jacs.5b01555
J. Am. Chem. Soc. 2015, 137, 6577–6586

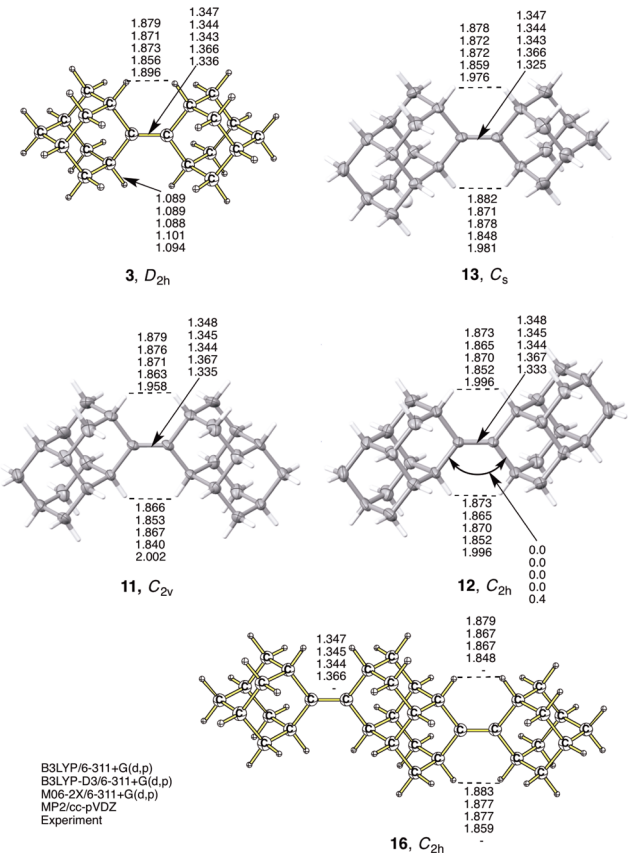

Figure 2. Experimental X-ray crystal structures (where available) as well as B3LYP/6-311+G(d,p), B3LYP-D3/6-311+G(d,p), M06-2X/6-311+G(d,p), and MP2/cc-pVDZ optimized structures (selected bond lengths in Å) of 2-(2-adamantylidene)adamantane (**3**), *syn*-3-(3-diamantylidene)diamantane (**11**), *anti*-3-(3-diamantylidene)-diamantane (**12**), 3-(2-adamantylidene)diamantane (**13**), and 3,10-bis-2-adamantylidene)diamantane (**16**) and the torsion angles in degrees.

density vectors,[35] the intramolecular H···H contacts around the C=C bond in **11**–**13** are significantly shorter (1.848–2.002 Å) than the sum of the hydrogen van der Waals radii (ca. 2.4 Å[36]). Although this should cause some strain, only marginal C=C bond twisting (up to 0.4° in **12**) is observed.

In order to judge the role of the intermolecular noncovalent interactions in the dimer structures we optimized them utilizing various DFT levels of theory, namely "conventional" B3LYP and B3LYP-D3[37] with Grimme's D3-dispersion correction. We compare these results with M06-2X[38] that was extensively parametrized for medium-range electron correlation, as well as with ab initio method MP2. For the diamondoid dimers all levels of theory, especially MP2, somewhat overestimate the experimental central C=C bond length by 0.01–0.03 Å (although theoretical r_e values are expected to be shorter than experiment).

As expected, B3LYP-D3 and M06-2X "tighten" the diamondoid dimers upon optimization, although the changes are small. We conclude that although the intramolecular H···H distances are not optimal (in terms of vdW-distance) this does not lead to twisting of the double bonds of the cage dimers. This situation is similar to tetraisopropyl ethylene, which retains its planarity despite formally high crowding.[39−42] These findings can be rationalized on the basis that even at much shorter distances, the H···H interactions are *still* stabilizing on the vdW-potential.[43]

Radical Cations. While the deviation from the planarity is typical only for highly crowded alkenes, it is characteristic for their ionized states, owing to partial loss of π-bonding. The prototypical system is ethylene,[44] which changes its symmetry from D_{2h} to D_{2d} upon ionization with a 27° double bond twist resulting from the balance between favorable π-bonding in the planar form and $\sigma-\pi$ hyperconjugation in the perpendicular orientation.[45] Such a distortion was first observed experimentally through the X-ray structural analysis of the long-lived sesquihomoadamantene radical cation that is an isomer of **3**.[46,47] The deviation from planarity in radical cations also depends on the substituents around the olefinic moiety and is much higher when bulky groups are present. For instance, crowding causes ca. 55° (M06-2X/cc-pVTZ) twisting in the persistent bis-2,2,5,5-tetramethylcyclopentylidene radical cation.[48] Moderately crowded 2-(2-adamantylidene)adamantane radical cation $\mathbf{3}^{\bullet+}$[26,27] is a good model for analyzing the influence of substitution on the distortion of the ionized states of alkenes as well as for benchmarking the computational methods (the experimental ionization potential of **3** is well established).[25] We first optimized the structure of $\mathbf{3}^{\bullet+}$ at various levels of theory. Previous computations at B3LYP/aug-cc-pVTZ[49] gave a C=C bond length of 1.419 Å. This agrees well with our B3LYP and M06-2X computations that give 1.411 ± 0.004 Å; MP2 with a cc-pVDZ and a cc-pVTZ basis set provide 1.429 and 1.417 Å, respectively. The C=C bond in $\mathbf{3}^{\bullet+}$, where ca. 70% of the NBO spin density and positive charge is located, is twisted by 24.0° ± 4.0°, which is typical for tetrasubstituted alkene radical cations.[50] The rest of the spin density is almost equally distributed among all carbon atoms; the remaining positive charge is located on the tertiary carbons. Such spin/charge distributions display a high degree of delocalization in $\mathbf{3}^{\bullet+}$.

Note that the noncovalent intramolecular H···H contact distances increase slightly in $\mathbf{3}^{\bullet+}$ (up to 0.2 Å) due to C=C bond twisting and elongation (Figure 3). The computational methods employed here reproduce the adiabatic ionization potential (IP_a) of **3**[51] very well (Table 2).

Inclusion of dispersion corrections with or without Becke–Johnson (BJ) damping (B3LYP-D3(BJ))[43] does not alter the results. The M06-2X functional shows satisfactory results even with double-ζ basis sets demonstrating only modest basis-set dependence. The MP2 computations overestimate the experimental value slightly and show negligible spin contamination ($\langle S^2\rangle$ = 0.760). As we recently determined[23] the ionization potentials of dimers **12** and **13** experimentally, we include these hydrocarbons in our computations as well (Table 3 and Figure 3). Their geometrical distortions (twisting) upon ionization are very close to that in **3**, and we note that among the DFT methods tested, M06-2X with a triple-ζ quality basis sets satisfactorily reproduces the IPs of C=C bond dimers **12** and **13**.

The situation is quite different when two π-bonds are connected by rigid diamondoid framework as in **16**. The prototypical case of 2,6-bis-methyleneadamantane (**17**) has been the focus of several studies.[52−56] The D_{2d}-symmetric ground state of **17** is subject to Jahn–Teller distortion upon ionization due to the presence of a doubly degenerated HOMO, and it is believed[56] that this molecule displays intramolecular electron transfer (ET) dynamics between two localized states $\mathbf{17a}^{\bullet+}$ and $\mathbf{17b}^{\bullet+}$ (Figure 4).

DOI: 10.1021/jacs.5b01555
J. Am. Chem. Soc. 2015, 137, 6577–6586

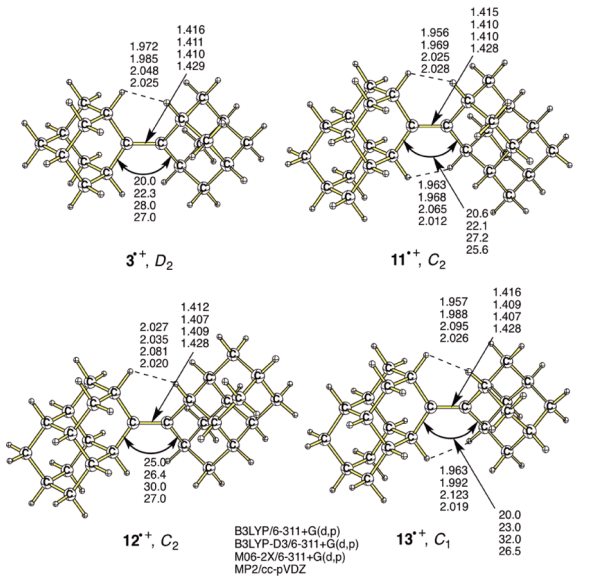

Figure 3. B3LYP/6-311+G(d,p), B3LYP-D3/6-311+G(d,p), M06-2X/6-311+G(d,p), and MP2/cc-pVDZ optimized structures (selected bond lengths in Å) of radical cations of 2-(2-adamantylidene)-adamantane ($3^{\bullet+}$), *syn*-3-(3-diamantylidene)diamantane ($11^{\bullet+}$), *anti*-3-(3-diamantylidene)diamantane ($12^{\bullet+}$), 3-(2-adamantylidene)-diamantane ($13^{\bullet+}$), and torsion angles in degrees.

Table 2. Computed Adiabatic Ionization Potentials (IP_a) of 2-(2-Adamantylidene)adamantane (3) at Various DFT and ab Initio Levels of Theory

method	basis	IP_a, eV
B3LYP	6-31G(d,p)	7.04
	cc-pVDZ	7.18
	6-311+G(d,p)	7.21
	cc-pVTZ	7.20
B3LYP-D3(BJ)	6-31G(d,p)	7.03
	cc-pVDZ	7.17
M06-2X	6-31G(d,p)	7.29
	cc-pVDZ	7.37
	cc-pVTZ	7.37
	6-311+G(d,p)	7.37
MP2	cc-pVDZ	7.59
	cc-pVTZ	7.74
experiment[51]		7.30

Table 3. Computed Adiabatic Ionization Potentials (IP_a, eV) of Dimers 12 and 13 at Various DFT and ab Initio Levels of Theory[a]

	B3LYP	M06-2X		MP2	
no.	6-311+G(d,p)	6-311+G(d,p)	cc-pVTZ	cc-pVDZ	exp.[23]
12	7.05 (C_2)	7.16 (C_1)	7.29 (C_1)	7.48 (C_1)	7.32
13	7.15 (C_1)	7.39 (C_1)	7.36 (C_1)	7.56 (C_1)	7.43

[a]Point groups in parentheses.

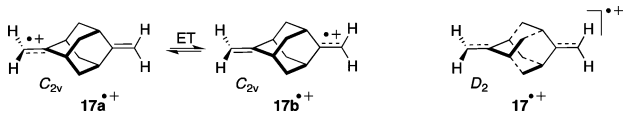

Figure 4. Two localized (C_{2v}) and delocalized (D_2) states of the 2,6-bis-methyleneadamantane radical cation $17^{\bullet+}$.

Ab initio semiclassical dynamics[54] as well as some DFT methods[56] show that the C_{2v} structure is not a minimum, while the D_2-structure is a very "shallow minimum",[54] and it was stated that the D_{2d}-structure is the "ground state global minimum energy structure" for $17^{\bullet+}$.[56] It was concluded, however,[54] that structural studies on $17^{\bullet+}$ are still tentative due to the low computational levels employed. In contrast, we have found that **17** forms a highly delocalized radical cation of D_2-symmetry, whose deviation from D_{2d} symmetry, however, is negligible (Figure 5): All DFT (M06-2X, B3LYP, B3LYP-D3,

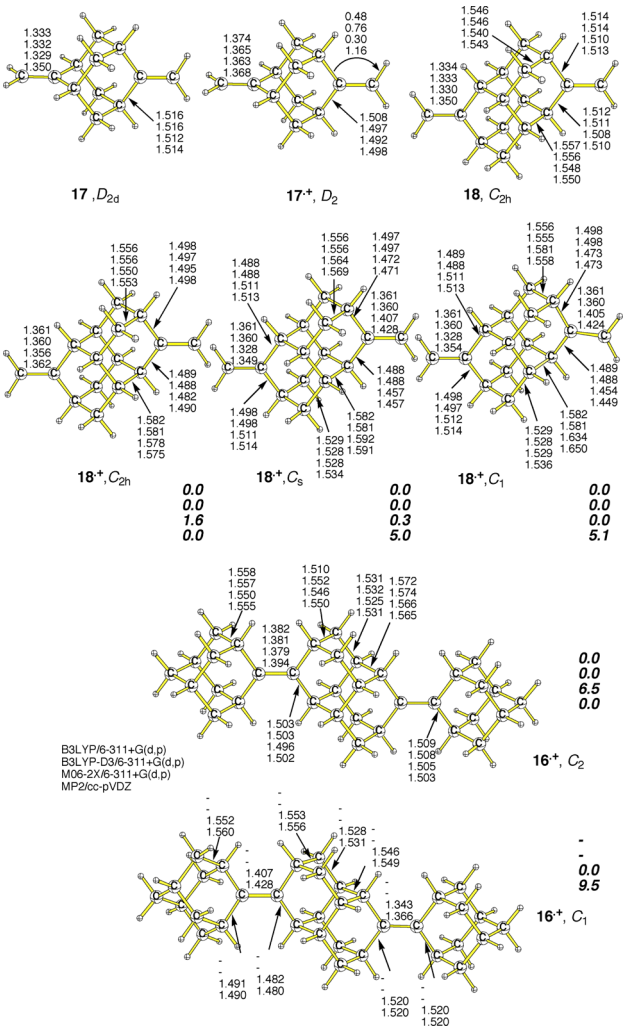

Figure 5. B3LYP/6-311+G(d,p)-, B3LYP-D3/6-311+G(d,p), M06-2X/6-311+G(d,p), and PMP2/cc-pVDZ optimized structures (selected bond lengths in Å) of 2,6-bis-methyleneadamantane ($17^{\bullet+}$), 3,10-bis-methylenediamantane ($18^{\bullet+}$), and different forms of 3,10-bis-2-adamantylidene)diamantane ($16^{\bullet+}$) radical cations. Relative energies (ΔE_0) of radical cation isomers in bold italics.

B3LYP-D3(BJ), mPW3PBE, BHandHLYP, LC-BLYP, ωB97, ωB97XD, and LC-ωPBE) methods as well as MP2 with various types of triple-ζ quality basis sets identify D_2-symmetric $17^{\bullet+}$ as a minimum with a torsional angle deviation less than 2° from the planar D_{2d}-symmetric structure. We also optimized the C_2 and C_{2v} symmetric structures that represent localized forms of $17^{\bullet+}$ with one electron-depleted C=C bond (Figure 4). However, these structures appear to be transition states at all levels of theory employed. We conclude that the adamantane cage effectively provides delocalization of spin and charge

DOI: 10.1021/jacs.5b01555
J. Am. Chem. Soc. 2015, 137, 6577−6586

within entire molecule: From the NBO analysis ca. 50% of positive charge and 30% of spin density localized on the CH_2 and CH groups of the adamantane moiety. This is in line with our previous studies on the ionized adamantane,[57] diamondoids and other cage compounds[58] that form highly delocalized radical cations displaying several elongated C—C and C—H bonds and high degree of spin/charge delocalization.

Table 4. Computed Adiabatic Ionization Potential (IP_a) of 2,6-bis-Methyleneadamantane (17) at Various DFT and ab Initio Levels of Theory

method	basis	IP_a (eV)
B3LYP	6-31G(d,p)	8.04
	6-311+G(d,p)	8.27
	cc-pVDZ	8.16
	cc-pVTZ	8.24
B3LYP-D3(BJ)	6-31G(d,p)	8.04
	cc-pVDZ	8.17
M06-2X	6-31G(d,p)	8.70
	cc-pVDZ	8.79
	cc-pVTZ	8.85
MP2	cc-pVDZ	8.61
	cc-pVTZ	8.81

The next larger representative, 3,10-bis-methylenediamantane (**18**), belongs to the nondegenerate C_{2h} point group and may therefore retain its symmetry upon ionization (Figure 5). The computations on C_{2h}-**18**$^{\bullet+}$, which is not subject to primary Jahn−Teller distortion, are instructive for predicting of the behavior of **16** upon ionization. Taking into account that the double bonds of **18** are located at larger distances than in **17**, the question arises whether the diamantane cage will be able to participate in charge and spin delocalization or whether the molecule will undergo secondary distortions from C_{2h} to lower symmetry. At many DFT levels (B3LYP, B3LYP-D3, ωB97XD, BHandHLYP, LC-ωPBE, and mPW3PBE) with a 6-311+G(d,p) basis set all forms of **18**$^{\bullet+}$ converge to a highly delocalized C_{2h}-structure with ca. 60% spin density located on the terminal carbon atoms of both C═CH_2 moieties. At M06-2X, however, we found several low-symmetry stationary points, in particular, a low-lying C_1-structure with one localized double bond (Figure 5). We conclude that, in contrast to **17**, the C═C bonds in **18** are fairly isolated by the large diamantane cage and the situation with trimer **16** may be similar.

Indeed, we found that at B3LYP/6-311+G(d,p) and cc-pVTZ **16** forms a highly delocalized radical cation (Figure 5) retaining the symmetry of the neutral. However, although C_{2h}-**16**$^{\bullet+}$ is a minimum at B3LYP/6-311+G(d,p) and MP2/cc-pVDZ we were able to locate alternative, localized structures with one electron-depleted C═C bond. In particular, we found that the C_1-minimum at MP2 is, however, ca. 9 kcal mol^{-1} higher in energy than the delocalized C_2-structure (Figure 5). In contrast, the distorted C_1 structure of **16**$^{\bullet+}$ is ca. 6 kcal mol^{-1} more favorable than the C_2-form at M06-2X, ωB97XD/6-311+G(d,p), and BHandHLYP.

Hence, the results for **16**$^{\bullet+}$ are very method sensitive and currently inconclusive. We thus tested even more DFT functionals (SI Table S8) for describing the ionized states of **16** by probing their ability to reproduce the IPs available from XPS-studies.[23] We again found that M06-2X reproduces the experimental values well if the localized C_1-structure of **16**$^{\bullet+}$ is considered; the IPs computed for the delocalized C_2-forms slightly differ from the experimental values.

Large Unsaturated Diamondoid Clusters As Models for the Electronic Properties of Self-Assembled Structures. As intermolecular attractions[13] determine the formation of self-assembled monolayers (SAMs) on surfaces, we computed a number of van der Waals complexes derived from unsaturated diamondoid dimers. We used the Grimme dispersion corrected B3LYP-D3 approach with BJ-damping as well as the M06-2X functional, which demonstrated superior performance in describing the electronic properties of diamondoid oligomers (*vide infra*). Owing to the system sizes we limited our studies to neutral and charged dimeric and tetrameric structures. Due to numerous H···H and H···C attractions between the CH surfaces,[59] neutral **12** forms a strongly bound (8.1 at M06-2X/cc-pVDZ and 9.0 kcal mol^{-1} at B3LYP-D3(BJ)/cc-pVDZ) dispersion dimer **19** (Figure 6).

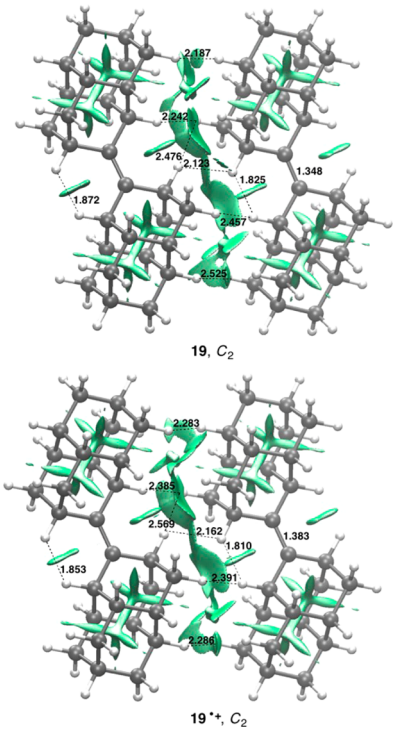

Figure 6. B3LYP-D3(BJ)/cc-pVDZ optimized geometries of the neutral *anti*-3-(3-diamantylidene)diamantane dimer (**19**) and its radical cation **19**$^{\bullet+}$ (selected interatomic distances in Å). The noncovalent attraction isosurfaces (NCI) are shown in green.

This is also characteristic for **3** (not shown), for which the complexation enthalpies are 5.5 and 7.6 kcal mol^{-1}, respectively. Such type of dispersion attractions decisively stabilize (in the order of tens of kcal mol^{-1}) the extremely long (up to 1.71 Å) C−C bonds in singly bonded diamondoid dimers.[59] The attraction is maximized when the components of the C_2-symmetrical complex **19** are shifted relatively to each other, while keeping the C═C bonds parallel. For SAMs derived from **12** the location such sp^2 "defects" relative to the surface will be determined by the position of the attachment points in **12** (*vide infra*) and is expected to be regular and well-defined. Important questions arise concerning the electronic properties of such clusters, e.g., how ionization, which is

DOI: 10.1021/jacs.5b01555
J. Am. Chem. Soc. 2015, 137, 6577−6586

relevant for molecular electronics applications, affects their structures and stabilities.[60]

To our surprise, besides a slight elongation (from 1.348 to 1.383 Å) and twisting (<4°) of the C═C bonds, only little geometrical changes occur upon ionization of **19** (Figure 6). In particular, the H···H contact distances remain almost unchanged in $\mathbf{19}^{\bullet+}$. This finding is supported through the comparison of the noncovalent attraction isosurfaces (NCI) for both the neutral and cationic forms (Figure 6). The interaction surfaces also emphasize that although the H···H contacts around the central double bonds are short (Figure 6), the interactions are still *attractive*, in line with the shape of the vdW-potential (which is still binding in the 1.8 Å region). Retaining C_2 symmetry for both the neutral and the radical cation implies that spin and charge delocalization of the latter is nearly perfect, a finding that is typically only associated with fully conjugated systems such as extended aromatics. As we have noted earlier,[58] the periplanar C—C bonding diamondoid framework allows strong hyperconjugative overlap through the *entire* cage (σ-conjugation), akin to the p-overlap found in extended conjugated π-systems, as recognized by Dewar in saying that "*there is no basic difference between saturated molecules and ones containing conjugated multiple bonds*".[61]

The fact that $\mathbf{19}^{\bullet+}$ retains the symmetry and the key geometrical parameters of the neutral suggests that SAMs constructed from diamondoid unsaturated dimers will be stable upon partial ionization or during electron-transfer processes. The same situation is found for the respective tetramer of **12** (see Table of contents graphics and SI for details), whose radical cation retains the C_2-symmetry of the neutral. We conclude that unsaturated diamondoid oligomers are highly promising for the construction of self-assembled structures that mimic hydrogen-terminated diamond surfaces where the presence of unsaturation aids in the electron/hole transfer processes.

Functionalization of Diamondoid Dimers. The potential use of diamondoid dimers in the construction of nanoelectronic devices is determined by the ability to deliver the electric charge to the molecule through proper functional group attachment points (SH, OH etc.).[9] The position of the functional group is decisive, as we have previously demonstrated that tertiary apical diamondoid derivatives form well-ordered SAMs with bonding energies exceedingly higher than those of medial ones.[27] The presence of a double bond in the above dimers determines (and limits) the choice of the functionalization method. Remarkably, while the reaction of **3** with bromine resulted in an isolable bromonium cation,[62] a *sec*-CH-substitution product **20** forms in the reaction with *N*-bromosuccinimide (NBS, Scheme 2) under aprotic conditions.[63] Bulky trihalomethyl ($^{\bullet}CHal_3$) radicals, on the other hand, provide high selectivities for tertiary positions as shown for the halogenations of adamantane.[64] For instance, $^{\bullet}CHal_3$ radicals can conveniently be generated under phase-transfer conditions (PTC) in the CBr_4/NaOH system.[65] This additionally prevents the formation of bromo-radicals that often form from the homolysis of halomethanes. Indeed, we were able to produce *tert*-bromide **21** in 52% preparative yield utilizing microwave acceleration.[66] Not even trace amounts of secondary bromo derivatives formed and unreacted **3** was quantitatively recovered (Scheme 2). This confirms the initial suggestion that the formation of 4-halo derivatives of **3** with NBS is an ionic process,[63] as our radical halogenations occur on the 5-position exclusively. This is in agreement with the fact

Scheme 2. Functionalizations of Dimers 3, 11, and 12 (Yields are Preparative)

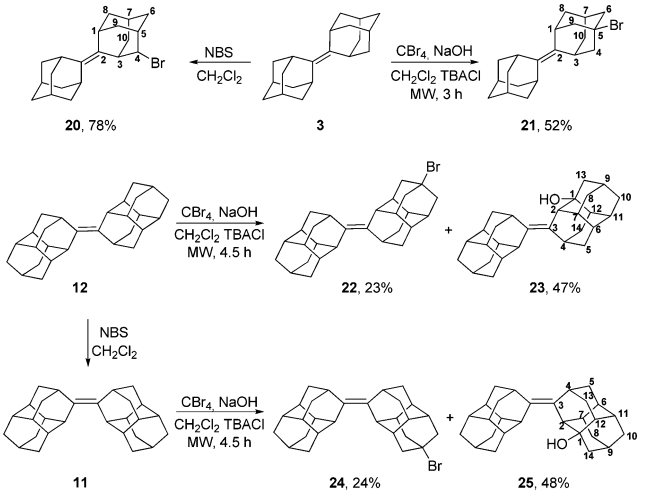

that *anti*-dimer **12** in the presence of NBS isomerizes to *syn*-isomer **11** as a result from the reversible attack of positivated bromine on the double bond. We thus applied the above PTC protocol for the bromination of dimers **11** and **12** and achieved almost complete conversion of the starting materials after 4.5 h at 70 °C that gives mixtures of bromides and alcohols. The structural assignments of the *tert*-bromides **22** and **24** are based on comparative analyses of ^{1}H and ^{13}C NMR spectra (for detailed analysis see the SI). C_s-Symmetry of the monobromides was confirmed by the presence of 20 signals in their ^{13}C NMR spectra. The choice between four alternative C_s-structures for apical bromides **22** and **24** was based on the presence three CH_2-groups downshifted due to the anisotropy of the bromo substituent. The ^{13}C NMR spectra indicate C_1 point groups of alcohols **23** and **25**, for which the positions of the OH-groups were identified through COSY-NMR experiments. For **23**, one of the low-field C═C—^{7}CH signals correlates with only one proton and displays W-type coupling with two different CH_2-groups ($^3CH_2$ and $^5CH_2$) as well as with the C═C—^{9}CH proton. The same correlations were observed for **25**. All derivatives were also characterized by comparative analysis of 2D (COSY, HSQC, and HMBC-TOCSY) spectra (see SI for details).

The fact that a mixture of apical bromides and medial alcohols forms simultaneously may be explained by the relative hydrolytic stabilities of the bromides. It is well established that the rate of solvolysis correlates well with the carbocation stabilities.[67] As the medial cations derived from **11** and **12** are ca. 6 kcal mol^{-1} (B3LYP/6-311+G(d,p)) more stable than the apical cations, this explains the relatively low hydrolytic stability of the medial bromides formed as intermediates in the PTC bromination.

■ CONCLUSIONS

We developed a simple and convenient procedure for the preparation of large C═C coupled diamondoid dimers as well as trimers of different sizes and shapes as possible candidates for the construction of diamond-like electronic materials. In the course of our investigation that is accompanied by chemical computations, we also probed the ability of modern DFT functionals to describe the neutral and ionized states of the diamondoid dimers and trimers. DFT generally seems to be

DOI: 10.1021/jacs.5b01555
J. Am. Chem. Soc. 2015, 137, 6577−6586

quite suitable in reproducing the experimental geometries of the neutrals and the first ionization potentials to the corresponding radical cations; the more modern M06-2X method in conjunction with double and triple-ζ basis sets appears to be slightly superior to B3LYP or ab initio MP2. The inclusion of explicit dispersion corrections does not alter these conclusions. As the ionized states of diamondoid vdW-complexes are tightly bound and able to delocalize charge and spin, the unsaturated oligomers are indeed suitable models for mimicking the electronic properties of H-terminated diamond surfaces with sp^2-defects.

For the functionalization with attachment points for metal surfaces we studied the C—H-bond substitution reactions of the diamondoid dimers. We were able to introduce substituents both in the medial and apical cage positions without touching the central double bond through a microwave-accelerated phase-transfer C—H-bond halogenation protocol.

As many of the desirable properties of diamond itself may derive from surface defects, the present study is a step in the direction of understanding such properties through a bottom-up approach. Furthermore, in marked contrast to the highly variable qualities of natural or man-made diamond, diamondoids are chemically pure so that clean-cut, reproducible experiments and solid quantification of their properties are possible.

Surfaces with diamondoids have already been prepared and published,[14,16,68] and we show here in much detail that the delocalization of charge and spin occurs not only within "defect" diamond assemblies, but also between them. The computations on the tetrameric van der Waals clusters leave little doubt that this also occurs within larger assemblies translating well the properties of the small isolated clusters onto diamondoid assemblies.

EXPERIMENTAL SECTION

All computations were performed with the GAUSSIAN09 program suite[69a] utilizing analytical first and second energy derivatives. The noncovalent interaction isosurfaces where ploted utilizing the NCIPLOT.[69b,c] The NMR spectra were recorded with a Bruker Advance II spectrometer, the chemical shifts are given in ppm relative to TMS. GC—MS analyses were performed with an HP5890 GC with an HP5971A mass-selective detector. High resolution mass spectra were recorded on a Finnigan MAT 95 instrument. Full experimental details with spectroscopic characterization of new compounds are provided in the SI.

3,10-Diamantanedione (7) and 3,8-Diamantanedione (10). 3.5 g of the mixture of the hydroxyketones (**9**) was stirred with H_2SO_4 (35 mL of 98%) at 75−77 °C for 7 days. The reaction mixture was poured onto ice, extracted with chloroform (4 × 50 mL), the combined extracts were washed with water (3 × 50 mL), brine (1 × 50 mL), dried over Na_2SO_4, and concentrated under reduced pressure. Separation of the residue by column chromatography on silica gel with pentane/ether (1/1) gave 1.38 g (40%) of 3,10-diamantanedione (**7**) and 0.62 g (15%) of 3,8-diamantanedione (**10**).

3,10-Diamantanedione (7). Mp = 236−237 °C. ^{1}H NMR ($CDCl_3$): 2.67 (bs, 2H), 2.58 (bs, 2H), 2.22 (bs, 4H), 2.14−1.98 (m, 8H). ^{13}C NMR: 215.2 (C), 54.2 (CH), 43.1 (CH), 38.2 (CH), 36.6 (CH_2). MS (*m*/*z*): 217 (12%), 216 (100%), 131 (30%), 117 (48%), 91 (84%), 79 (56%). HR−MS: found 216.1151 (calculated for $C_{14}H_{16}O_2$ 216.1150).

3,8-Diamantanedione (10). Mp = 254−255 °C. ^{1}H NMR ($CDCl_3$): 2.70 (s, 2H), 2.59 (s, 2H), 2.21−2.12 (m, 8H), 2.12−1.99 (m, 4H). ^{13}C NMR: 213.2 (C), 55.9 (CH), 43.7 (CH), 38.9 (CH), 38.0 (CH_2), 37.6 (CH_2), 35.5 (CH). MS (*m*/*z*): 217 (14%), 216 (100%), 188 (10%), 117 (15%), 91 (18%). HR−MS: found 216.1152 (calculated for $C_{14}H_{16}O_2$ 216.1150).

9-Hydroxy-3-diamantanone (8). HNO_3 (100%, 20 mL) was added to a solution of diamantanone (10 g, 53.2 mmol) in methylene chloride (50 mL) at 0 °C under stirring. The reaction mixture was stirred for 48 h at rt and diluted with water (50 mL) under stirring. The methylene chloride was distilled off, and residual water solution was refluxed for 12 h. The cooled mixture was extracted with methylene chloride (5 × 50 mL), the combined organic extracts were washed with aq $NaHCO_3$ (2 × 50 mL), brine (2 × 50 mL), dried over Na_2SO_4, and concentrated under reduced pressure. Separation of the residue by column chromatography on silica gel (hexane/ethyl acetate = 1/1) gave 2.01 g (20%) of diamantanone (**5**), 3.67 g (34%) of 9-hydroxy-3-diamantanone (**8**) as a colorless solid and 4.53 g (42%) of a mixture of monohydroxy ketones (**9**).

9-Hydroxy-3-diamantanone (8). Mp = 191−192 °C. ^{1}H NMR (400 MHz, $CDCl_3$): 2.4 (bs, 1H), 2.35 (bs, 1H), 2.23 (bs, 1H), 2.1 (bs, 1H), 2.02−1.87 (m, 4H), 1.85−1.75 (m, 6H), 1.67−1.58 (m, 2H), 1.51 (bs, 1H). ^{13}C NMR: 217.5 (C), 66.7 (C), 54.3 (CH), 44.5 (CH_2), 44.0 (CH_2), 43.4 (CH), 42.2 (CH), 38.6 (CH), 37.5 (CH_2), 35.3 (CH). MS (*m*/*z*): 219 (14%), 218 (68%), 200 (15%), 190 (10%), 172 (25%), 133, 115 (23%), 107 (39%), 91 (100%), 79, 77 (87%), 55 (40%). Other characteristics of **8** are identical to those previously reported.[70]

Typical Coupling Procedure. A 100 mL two-necked dry flask equipped with a magnetic stirrer and a reflux condenser with a bubble counter was heated under argon, and 25 mL of freshly distilled dry THF were added through a septum. The solvent was cooled with an external ice bath and 1.35 mL (12.3 mmol) of $TiCl_4$ were added. The septum was removed, and Zn powder (1.62 g, 24.9 mmol) was added in small portions. After the Zn addition, the reaction mixture was refluxed for 1 h and then cooled to ambient temperature. The pyridine (0.5 mL) was added, followed by addition of a solution of ketone (5.34 mmol) in dry THF (7 mL). The mixture was refluxed under argon for 12 h, cooled to room temperature and quenched by dropwise addition of a 10% aq solution of K_2CO_3 (60 mL) with simultaneous cooling. The dark blue slurry was added to diethyl ether (150 mL), vigorously stirred for 15 min and then filtered. The residue was washed with diethyl ether (3 × 50 mL). The layers in the filtrate were separated, and the aqueous layer was extracted with diethyl ether (2 × 50 mL). The combined organic layers were washed sequentially water (1 × 70 mL), hydrochloric acid (5%, 2 × 50 mL), water (2 × 70 mL), and brine (1 × 50 mL). The organic layer was dried over Na_2SO_4 and the solvent was removed in vacuo. The residue was purified by column chromatography (hexane) to afford the olefin.

*syn-3-(3-Diamantylidene)diamantane (**11**).* Mp = 245−248 °C ^{1}H NMR ($CDCl_3$): 2.82 (s, 2H), 2.74 (s, 2H), 1.82−1.69 (m, 24H), 1.64−1.55 (m, 8H). ^{13}C NMR ($CDCl_3$): δ 133.9 (C), 41.3 (CH), 39.8 (CH_2), 39.3 (CH), 38.2 (CH_2, 2 signals), 37.8 (CH), 37.2 (CH), 29.5 (CH), 25.9 (CH). MS (*m*/*z*): 372 (100%), 291 (2%), 277 (4%), 187 (21%), 129 (6%), 91 (11%). HR−MS: found 372.2829 (calculated for $C_{28}H_{36}$ 372.2817).

*anti-3-(3-Diamantylidene)diamantane (**12**).* Mp = 276 °C. ^{1}H NMR ($CDCl_3$): 2.85 (s, 2H), 2.73 (s, 2H), 1.81−1.70 (m,

DOI: 10.1021/jacs.5b01555
J. Am. Chem. Soc. 2015, 137, 6577−6586

24H), 1.65 (s, 4H), 1.62−1.56 (m, 4H). ^{13}C NMR ($CDCl_3$): 133.8 (C), 41.7 (CH), 39.9 (CH_2), 39.3 (CH), 38.2 (CH_2), 38.2 (CH_2), 37.8 (CH), 37.2 (CH), 29.1 (CH), 25.9 (CH). MS (*m*/*z*): 372 (100%), 291 (1%), 277 (3%), 221 (1%), 187 (20%), 129 (8%), 91 (13%). HR−MS: found 372.2820 (calculated for $C_{28}H_{36}$ 372.2817).

*3-(2-Adamantylidene)diamantane (**13**).* Mp = 168−169 °C ^{1}H NMR ($CDCl_3$): 2.94 (s, 1H), 2.91 (s, 1H), 2.80 (s, 1H), 2.72 (s, 1H), 1.94−1.89 (m, 2H), 1.87−1.72 (m, 17H), 1.70−1.54 (m, 9H). ^{13}C NMR ($CDCl_3$): 133.7 (C), 133.4 (C), 41.4 (CH), 39.8 (CH_2), 39.8 (CH_2), 39.7 (CH_2), 39.2 (CH), 38.2 (CH_2), 38.2 (CH_2), 37.8 (CH), 37.4 (CH_2), 37.2 (CH), 32.2 (CH), 31.8 (CH), 29.2 (CH), 28.6 (CH), 26.0 (CH). MS (*m*/*z*): 321 (26%), 320 (100%), 268 (8%), 263 (8%), 187 (10%), 135 (7%), 133 (8%), 119 (5%), 117 (7%), 111 (6%), 105 (9%), 97 (9%), 95 (8%), 93 (8%), 91 (16%) Anal: calculated for $C_{24}H_{32}$: C, 89.94; H, 10.06; found: C, 90.05; H, 10.15.

*8-(2-Adamantylidene)triamantane (**14**).* ^{1}H NMR ($CDCl_3$): 2.94 (s, 1H), 2.90 (s, 1H), 2.85 (s, 1H), 2.65 (s, 1H), 1.92 (s, 2H), 1.88−1.80 (m, 7H), 1.77−1.59 (m, 16H), 1.58−1.52 (m, 2H), 1.36−1.28 (m, 3H), 1.23−1.15 (m, 2H). ^{13}C NMR ($CDCl_3$): 133.5 (C), 133.4 (C), 48.2 (CH), 46.9 (CH_2), 46.6 (CH), 45.1 (CH_2), 41.9 (CH), 39.8 (CH_2), 39.8 (CH_2), 39.7 (CH_2), 39.7 (CH_2), 39.7 (CH_2), 38.5 (CH_2), 38.4 (CH), 38.2 (CH), 38.2 (CH_2), 38.0 (CH), 38.0 (CH_2), 37.4 (CH_2), 36.9 (CH), 35.3 (CH), 33.8 (C), 32.1 (CH), 32.0 (CH), 31.1 (CH), 28.6 (CH), 28.6 (CH), 27.8 (CH). MS (*m*/*z*): 373 (31%), 372 (100%), 239 (22%), 207 (10%), 186 (10%), 179 (10%), 178 (10%), 169 (10%), 167 (17%), 165 (21%), 159 (11%), 158 (13%), 157 (10%), 152 (10%), 143 (28%), 142 (10%), 141 (34%), 135 (17%), 133 (23%), 132 (12%), 131 (34%), 130 (14%), 129 (70%), 128 (45%), 121 (14%), 119 (34%), 117 (43%), 116 (22%), 115 (27%), 109 (13%), 107 (22%), 105 (69%), 103 (12%), 95 (14%), 93 (43%), 92 (15%), 91 (94%), 81 (31%), 79 (58%), 78 (10%), 77 (18%), 67 (20%), 55 (18%). Anal: calculated for $C_{28}H_{36}$: C, 90.26; H, 9.74; found: C, 90.13; H, 9.58.

*8-(8-Triamantylidene)triamantane (**15**).* Mp = 304−305 °C. ^{1}H NMR ($CDCl_3$): 2.87 (s, 2H), 2.62 (s, 2H), 1.81 (s, 2H), 1.75−1.55 (m, 26H), 1.42−1.17 (m, 12H). ^{13}C NMR ($CDCl_3$): 133.7 (C), 48.2 (CH), 47.0 (CH_2), 46.6 (CH), 45.1 (CH_2), 42.1 (CH), 39.8 (CH_2), 38.5 (CH_2), 38.4 (CH), 38.3 (CH), 38.2 (CH_2), 38.1 (CH), 38.0 (CH_2), 37.0 (CH), 35.3 (CH), 33.8 (C), 31.1 (CH), 27.8 (CH). MS (*m*/*z*): 476 (100%), 341 (1%), 238 (100%), 217 (2%), 183 (3%), 143 (4%), 129 (13%). HR−MS: found 476.3438 (calculated for $C_{36}H_{44}$ 476.3443).

*Bis-(2-adamantylidene)diamantane-3,8 (**16**).* Mp = 345−347 °C. ^{1}H NMR ($CDCl_3$): 2.95 (s, 2H), 2.89 (s, 2H), 2.80 (s, 2H), 2.76 (s, 2H), 1.95−1.76 (m, 20H), 1.72−1.59 (m, 16H).^{13}C NMR ($CDCl_3$): 133.7 (C), 133.5 (C), 41.2 (CH), 40.0 (CH_2), 39.95 (CH_2), 39.92 (CH_2), 39.7 (CH), 37.7 (CH_2), 32.5 (CH), 32.2 (CH), 29.5 (CH), 29.0 (CH). MS (*m*/*z*): 452 (100%). HR−MS: found 452.3420 (calculated for $C_{34}H_{44}$ 452.3443).

General procedure for the functionalization of dimers under PTC conditions.

Carbon tetrabromide (0.52 g), aq sodium hydroxide (50%, 1.1 mL), tetra-*n*-butylammonium bromide (10 mg) were added to a solution of the dimer (0.54 mmol) in methylene chloride (3.1 mL). The reaction mixture was stirred for 3−4.5 h at 70 °C (200W, microwave), poured into water (10 mL) and extracted with methylene chloride (3 × 10 mL). The combined organic layers were washed with brine (3 × 5 mL), dried over Na_2SO_4, and the solvent was removed in vacuo. Separation of the residue by column chromatography on silica gel with pentane gave corresponding bromides and changing the eluent to pentane/ether = 1/1 provided the alcohols. The last fractions were additionally recrystallized from hexane to afford pure alcohols.

*5-Bromo-2-(2-adamantylidene)adamantane (**21**).* Mp = 125−127 °C. ^{1}H NMR ($CDCl_3$): 3.07 (s, 2H), 2.87 (s, 2H), 2.45 (s, 2H), 2.45−2.40 (m, 4H), 2.24−2.28 (m, 2H), 2.17 (m, 1H), 1.89−1.79 (m, 8H), 1.71−1.61 (m, 6H). ^{13}C NMR ($CDCl_3$): 136.0 (C), 129.0 (C), 66.9 (C), 50.7 (CH_2), 49.0 (CH_2), 39.5 (CH_2), 39.5 (CH_2), 37.5 (CH_2), 37.2 (CH_2), 35.7 (CH), 33.0 (CH), 32.1 (CH), 28.4 (CH), 28.3 (CH). MS (*m*/*z*): 348 (36%), 346 (37%), 268 (21%), 267 (97%), 225 (14%), 212 (18%), 211 (100%), 135 (19%), 129 (13%), 119 (16%), 117 (11%), 105 (15%), 93 (17%), 91 (39%), 81 (12%), 79 (23%). Anal: calcd for $C_{20}H_{27}Br$: C, 69.16; H, 7.84; found: C, 69.14; H, 7.91.

*9-Bromo-anti-3-(3-diamantylidene)diamantane (**22**).* Mp = 251−252 °C. ^{1}H NMR ($CDCl_3$): 2.88 (s, 1H), 2.83 (s, 2H), 2.74 (s, 1H), 2.42−2.34 (m, 6H), 1.98 (s, 1H), 1.88 (s, 2H), 1.85 (s, 2H), 1.83−1.78 (m, 8H), 1.76−1.72 (m, 6H), 1.66−1.55 (m, 6H). ^{13}C NMR ($CDCl_3$): 135.6 (C), 131.6 (C), 65.9 (C), 49.6 (CH_2), 49.5 (CH_2), 43.3 (CH), 41.8 (CH), 41.1 (CH), 39.9 (CH), 39.8 (CH_2), 39.2 (CH), 38.7 (CH_2), 38.14 (CH_2), 38.12 (CH_2), 37.6 (CH), 37.0 (CH), 36.0 (CH), 29.3 (CH), 28.6 (CH), 25.9 (CH). MS (*m*/*z*): 452 (20%), 450 (20%), 371 (19%), 205 (10%), 187 (18%), 165 (15%), 154 (23%), 141 (11%), 129 (17%), 117 (21%), 105 (28%), 91 (100%), 79 (87%), 67 (35%), 55 (40%). HR−MS: found 450.1909 (calculated for $C_{28}H_{35}Br$ 450.1922).

*1-Hydroxy-anti-3-(3-diamantylidene)diamantane (**23**).* Mp = 280−282 °C. ^{1}H NMR ($CDCl_3$): 2.91 (s, 1H), 2.86 (s, 1H), 2.82 (s, 1H), 2.71 (s, 1H), 2.22 (s, 1H), 2.14 (s, 1H), 2.05 (s, 1H), 1.96−1.90 (m, 2H), 1.90−1.85 (m, 1H), 1.85−1.80 (m, 5H), 1.80−1.66 (m, 15H), 1.65 (s, 2H), 1.63−1.55 (m, 4H). ^{13}C NMR ($CDCl_3$): 140.8 (C), 129.0 (C), 71.1 (C), 48.2 (CH), 43.6 (CH_2), 43.6 (CH) 42.1 (CH), 41.4 (CH), 40.2 (CH_2), 40.0 (CH_2), 39.7 (CH), 39.5 (CH), 39.3 (CH), 39.0 (CH_2), 38.0 (CH_2), 38.0 (CH_2), 38.0 (CH_2), 37.6 (CH), 37.4 (CH), 37.2 (CH_2, 2 signals), 37.0 (CH), 36.5 (CH), 34.8 (CH_2), 30.1 (CH), 29.2 (CH), 28.6 (CH), 25.8 (CH). MS (*m*/*z*): 388 (100%), 370 (17%), 187 (18%), 167 (10%), 157 (10%), 143 (12%), 129 (23%), 117 (19%), 105 (30%), 91 (77%), 79 (48%), 67 (3%1), 55 (35%). Anal: calculated for $C_{28}H_{36}O$: C, 86.54; H, 9.34; found: C, 86.70; H, 9.14.

*9-Bromo-syn-3-(3-diamantylidene)diamantane (**24**).* Mp = 173 °C. ^{1}H NMR ($CDCl_3$): 2.81 (s, 2H), 2.78 (s, 1H), 2.69 (s, 1H), 2.41−2.31 (m, 6H), 1.95 (s, 1H), 1.84 (s, 2H), 1.82−1.68 (m, 17H), 1.63−1.52 (m, 5H). ^{13}C NMR ($CDCl_3$): 135.2 (C), 131.3 (C), 65.5 (C), 49.3 (CH_2, 2 signals), 43.0 (CH), 41.2 (CH), 40.8 (CH), 39.4 (CH_2), 39.2 (CH), 39.0 (CH), 38.3 (CH_2), 37.8 (CH_2), 37.7 (CH_2), 37.3 (CH), 36.7 (CH), 35.7 (CH), 29.3 (CH), 28.6 (CH), 25.5 (CH). MS (*m*/*z*): 452 (15%), 450 (15%), 372 (64%) 371 (75%), 370 (46%), 287 (12%), 277 (17%), 275 (16%), 187 (50%), 165 (16%), 155 (17%), 143 (25%), 129 (52%), 117 (20%), 105 (63%), 91 (100%), 79 (45%), 67 (22%), 55 (29%). Anal: calculated for $C_{28}H_{35}Br$: C, 74.49; H, 7.81; found: C, 74.43; H, 7.75.

*1-Hydroxy-syn-3-(3-diamantylidene)diamantane (**25**).* Mp = 226−227 °C. ^{1}H NMR ($CDCl_3$): 2.83 (s, 1H), 2.74 (s, 1H), 2.71 (s, 1H), 2.64 (s, 1H), 2.22 (s, 1H), 2.06 (s, 1H), 1.95 (s,

DOI: 10.1021/jacs.5b01555
J. Am. Chem. Soc. 2015, 137, 6577−6586

1H), 1.88−1.81 (m, 2H), 1.79−1.46 (m, 27H). ^{13}C NMR ($CDCl_3$): 140.9 (C), 129.0 (C), 71.0 (C), 47.7 (CH), 43.6 (CH), 43.5 (CH_2), 41.4 (CH), 41.3 (CH), 40.1 (CH_2), 39.8 (CH_2), 39.7 (CH), 39.6 (CH), 39.5 (CH), 39.0 (CH_2), 38.0 (CH_2), 37.9 (CH_2, 2 signals), 37.6 (CH), 37.4 (CH), 37.23 (CH_2), 37.24 (CH_2), 37.0 (CH), 36.5 (CH), 34.8 (CH_2), 30.1 (CH), 30.0 (CH), 28.9 (CH), 25.8 (CH). MS (*m*/*z*): 388 (100%), 370 (22%), 277 (9%), 187 (15%), 167 (12%), 155 (8%), 141 (11%), 129 (22%), 117 (16%), 105 (38%), 91 (92%), 79 (72%). Anal: calculated for $C_{28}H_{36}O$: C, 86.54; H, 9.34; found: C, 86.39; H, 9.26.

Izomerization of *anti*-3-(3-Diamantylidene)-diamantane (12) with NBS. 0.12 g (0.7 mmol) of *N*-bromosuccinimide was added to a solution of 0.026 g (0.07 mmol) of *anti*-3-(3-diamantylidene)diamantane (**12**) in methylene chloride (2 mL). The reaction mixture was stirred at reflux for 24 h and controlled by GC−MS that showed the presence of an intractable mixture of bromides together with *syn*- and *anti*-3-(3-diamantylidene)diamantanes (**11** and **12**) as a 3:2 mixture.

■ ASSOCIATED CONTENT

Supporting Information

The copies of the NMR spectra and XYZ-coordinates of optimized species. The Supporting Information is available free of charge on the ACS Publications website at DOI: 10.1021/jacs.5b01555.

■ AUTHOR INFORMATION

Corresponding Authors

*prs@org.chemie.uni-giessen.de.
*aaf@xtf.kpi.ua.

Funding

This work was supported by the Deutsche Forschungsgemeinschaft (Schr 597/23−1) and Ukrainian Basic Research State Foundation.

Notes

The authors declare no competing financial interest.

■ REFERENCES

(1) Hokazono, A.; Ishikura, T.; Nakamura, K.; Yamashita, S.; Kawarada, H. *Diamond Relat. Mater.* **1997**, *6*, 339−343.
(2) Rouse, A. A.; Bernhard, J. B.; Sosa, E. D.; Golden, D. E. *Appl. Phys. Lett.* **1999**, *75*, 3417−3419.
(3) Hu, Y.; Shenderova, O. A.; Hu, Z.; Padgett, C. W.; Brenner, D. W. *Rep. Prog. Phys.* **2006**, *69*, 1847−1895.
(4) Kraft, A. *Int. J. Electrochem. Sci.* **2007**, *2*, 355−385.
(5) Smith, J. R.; Bilbro, G. L.; Nemanich, R. J. *Phys. Rev. B* **2007**, *76*, 245327.
(6) Gorelik, V. S.; Rakhmatullaev, I. A. *Inorg. Mater.* **2004**, *40*, 686−689.
(7) Schell, A. W.; Kewes, G.; Hanke, T.; Leitenstorfer, A.; Bratschitsch, R.; Benson, O.; Aichele, T. *Opt. Express* **2011**, *19*, 7914−7920.
(8) Gunawan, M. A.; Hierso, J.-C.; Poinsot, D.; Fokin, A. A.; Fokina, N. A.; Tkachenko, B. A.; Schreiner, P. R. *New J. Chem.* **2014**, *38*, 28−41.
(9) Schwertfeger, H.; Fokin, A. A.; Schreiner, P. R. *Angew. Chem., Int. Ed.* **2008**, *47*, 1022−1036.
(10) Shenderova, O. A.; Zhirnov, V. V.; Brenner, D. W. *Crit. Rev. Solid State Mater. Sci.* **2002**, *27*, 227−356.
(11) Kharisov, B. I.; Kharissova, O. V.; Chavez-Guerrero, L. *Synth. React. Inorg. Met.* **2010**, *40*, 84−101.
(12) Randel, J. C.; Niestemski, F. C.; Botello-Mendez, A. R.; Mar, W.; Ndabashimiye, G.; Melinte, S.; Dahl, J. E. P.; Carlson, R. M. K.; Butova, E. D.; Fokin, A. A.; Schreiner, P. R.; Charlier, J. C.; Manoharan, H. C. *Nature Comm.* **2014**, *5*, 4877.
(13) Willey, T. M.; Lee, J. R. I.; Fabbri, J. D.; Wang, D.; Nielsen, M. H.; Randel, J. C.; Schreiner, P. R.; Fokin, A. A.; Tkachenko, B. A.; Fokina, N. A.; Dahl, J. E. P.; Carlson, R. M. K.; Terminello, L. J.; Melosh, N. A.; van Buuren, T. *J. Electron Spectrosc. Relat. Phenom.* **2009**, *172*, 69−77.
(14) Li, F. H.; Fabbri, J. D.; Yurchenko, R. I.; Mileshkin, A. N.; Hohman, J. N.; Yan, H.; Yuan, H.; Tran, I. C.; Willey, T. M.; Bagge-Hansen, M.; Dahl, J. E. P.; Carlson, R. M. K.; Fokin, A. A.; Schreiner, P. R.; Shen, Z.-X.; Melosh, N. A. *Langmuir* **2013**, *29*, 9790−9797.
(15) (a) Drummond, N. D.; Williamson, A. J.; Needs, R. J.; Galli, G. *Phys. Rev. Lett.* **2005**, *95*, 096801. (b) Fokin, A. A.; Tkachenko, B. A.; Gunchenko, P. A.; Gusev, D. V.; Schreiner, P. R. *Chem.—Eur. J.* **2005**, *11*, 7091−7101.
(16) Yang, W. L.; Fabbri, J. D.; Willey, T. M.; Lee, J. R. I.; Dahl, J. E.; Carlson, R. M. K.; Schreiner, P. R.; Fokin, A. A.; Tkachenko, B. A.; Fokina, N. A.; Meevasana, W.; Mannella, N.; Tanaka, K.; Zhou, X. J.; van Buuren, T.; Kelly, M. A.; Hussain, Z.; Melosh, N. A.; Shen, Z. X. *Science* **2007**, *316*, 1460−1462.
(17) Burns, W.; McKervey, M. A.; Mitchell, T. R. B.; Rooney, J. J. *J. Am. Chem. Soc.* **1978**, *100*, 906−911.
(18) Burns, W.; Mitchell, T. R. B.; McKervey, M. A.; Rooney, J. J.; Ferguson, G.; Roberts, P. *J. Chem. Soc., Chem. Commun.* **1976**, 893−895.
(19) Dahl, J. E.; Liu, S. G.; Carlson, R. M. K. *Science* **2003**, *299*, 96−99.
(20) Hopf, H. *Angew. Chem., Int. Ed.* **2003**, *42*, 2000−2002.
(21) Geluk, H. W. *Synthesis* **1970**, *12*, 652−653.
(22) Recently, we prepared the sp^3−sp^3 9-(9-triamantyl)-triamantane dimer, which the largest diamondoid molecule known to date and whose dimension already approaches 1.5 nm (ref 59).
(23) (a) Meinke, R.; Richter, R.; Merli, A.; Fokin, A. A.; Koso, T. V.; Rodionov, V. N.; Schreiner, P. R.; Thomsen, C.; Maultzsch, J. *J. Chem. Phys.* **2014**, *140*, 034309(5p). (b) Zimmermann, T.; Richer, R.; Knecht, A.; Fokin, A. A.; Koso, T. V.; Chernish, L. V.; Gunchenko, P. A.; Schreiner, P. R.; Möller, T.; Rander, T. *J. Chem. Phys.* **2013**, *139*, 084310(6p).
(24) Banerjee, S.; Saalfrank, P. *Phys. Chem. Chem. Phys.* **2014**, *16*, 144−158.
(25) Nelsen, S. F.; Kessel, C. R. *J. Am. Chem. Soc.* **1979**, *101*, 2503−2504.
(26) Pichierri, F. *J. Mol. Struct. Theochem* **2004**, *668*, 179−187.
(27) Willey, T. M.; Fabbri, J. D.; Lee, J. R. I.; Schreiner, P. R.; Fokin, A. A.; Tkachenko, B. A.; Fokina, N. A.; Dahl, J. E. P.; Carlson, R. M. K.; Vance, A. L.; Yang, W. L.; Terminello, L. J.; van Buuren, T.; Melosh, N. A. *J. Am. Chem. Soc.* **2008**, *130*, 10536−10544.
(28) Claridge, S. A.; Liao, W. S.; Thomas, J. C.; Zhao, Y. X.; Cao, H. H.; Cheunkar, S.; Serino, A. C.; Andrews, A. M.; Weiss, P. S. *Chem. Soc. Rev.* **2013**, *42*, 2725−2745.
(29) Diamondoid oligomers **11**, **12**, **13**, **14**, and **15** were claimed to have been prepared as mentioned in U.S.A. Patent 5019660 "Diamondoid polymeric compositions", May 28, 1991. However, chemical or physical characterizations of these compounds was not reported nor was the patenting followed up by publications. Moreover, the synthesis of several ketones and polyketones presented as starting materials for the dimers and oligomers is, based on the new results presented here and our previous data (Fokin, A. A.; Zhuk, T. S.; Pashenko, A. E.; Dral, P. O.; Gunchenko, P. A.; Dahl, J. E. P.; Carlson, R. M. K.; Koso, T. V.; Serafin, M.; Schreiner, P. R. *Org. Lett.* **2009**, *11*, 3068−3071) rather unlikely, because the claimed isolation of "ketone fractions" is very challenging and has not been described in this patent.
(30) McMurry, J. E.; Fleming, M. P. *J. Am. Chem. Soc.* **1974**, *96*, 4708−4709.
(31) Marchand, A. P.; Reddy, G. M.; Deshpande, M. N.; Watson, W. H.; Nagl, A.; Lee, O. S.; Osawa, E. *J. Am. Chem. Soc.* **1990**, *112*, 3521−3529.

DOI: 10.1021/jacs.5b01555
J. Am. Chem. Soc. 2015, 137, 6577−6586

(32) Schaap, A. P.; Faler, G. R. *J. Org. Chem.* **1973**, *38*, 3061−3062.
(33) Fleming, M. P.; McMurry, J. E. *Org. Synth.* **1981**, *60*, 113−117.
(34) Allen, F. H.; Kennard, O.; Watson, D. G.; Brammer, L.; Orpen, A. G.; Taylor, R. *J. Chem. Soc., Perkin Trans. 2* **1987**, S1−S19.
(35) Rathore, R.; Lindeman, S. V.; Zhu, C. J.; Mori, T.; Schleyer, P. V. R.; Kochi, J. K. *J. Org. Chem.* **2002**, *67*, 5106−5116.
(36) Bondi, A. *J. Phys. Chem.* **1964**, *68*, 441−451.
(37) Grimme, S. *Org. Lett.* **2010**, *12*, 4670−4673.
(38) Zhao, Y.; Truhlar, D. G. *Theor. Chem. Acc.* **2008**, *120*, 215−241.
(39) Bomse, D. S.; Morton, T. H. *Tetrahedron Lett.* **1975**, 781−784.
(40) Casalone, G.; Pilati, T.; Simonetta, M. *Tetrahedron Lett.* **1980**, *21*, 2345−2348.
(41) Ermer, O. *Angew. Chem., Int. Ed.* **1983**, *22*, 998−1000.
(42) Langler, R. F.; Tidwell, T. T. *Tetrahedron Lett.* **1975**, 777−780.
(43) Grimme, S. *WIREs Comput. Mol. Sci.* **2011**, *1*, 211−228.
(44) Baker, A. D.; Baker, C.; Brundle, C. R.; Turner, D. W. *Int. J. Mass Spectrom. Ion Phys.* **1968**, *1*, 285−301.
(45) Mulliken, R. S.; Roothaan, C. C. J. *Chem. Rev.* **1947**, *41*, 219−231.
(46) Kochi, J. K.; Rathore, R.; Zhu, C. J.; Lindeman, S. V. *Angew. Chem., Int. Ed.* **2000**, *39*, 3671−3674.
(47) Kochi, J. K.; Rathore, R.; Zhu, C. J.; Lindeman, S. V. *Angew. Chem., Int. Ed.* **2001**, *40*, 278−278.
(48) Gerson, F.; Lopez, J.; Krebs, A.; Ruger, W. *Angew. Chem., Int. Ed.* **1981**, *20*, 95−96.
(49) Guerrero, A.; Herrero, R.; Quintanilla, E.; Davalos, J. Z.; Abboud, J. L. M.; Coto, P. B.; Lenoir, D. *ChemPhysChem* **2010**, *11*, 713−721.
(50) Takahashi, O.; Kikuchi, O. *J. Mol. Struct. Theochem.* **1994**, *119*, 207−218.
(51) M?llere, P. D.; Houk, K. N.; Bomse, D. S.; Morton, T. H. *J. Am. Chem. Soc.* **1976**, *98*, 4732−4736.
(52) Jones, G. A.; Carpenter, B. K.; Paddon-Row, M. N. *J. Am. Chem. Soc.* **1999**, *121*, 11171−11178.
(53) Blancafort, L.; Jolibois, F.; Olivucci, M.; Robb, M. A. *J. Am. Chem. Soc.* **2001**, *123*, 722−732.
(54) Blancafort, L.; Hunt, P.; Robb, M. A. *J. Am. Chem. Soc.* **2005**, *127*, 3391−3399.
(55) Janku, J.; Landa, S. *Coll. Czech. Chem. Comm.* **1970**, *35*, 375−377.
(56) Tavernelli, I. *J. Phys. Chem. A* **2007**, *111*, 13528−13536.
(57) Shubina, T. E.; Fokin, A. A. *WIREs Comput. Mol. Sci.* **2011**, *1*, 661−679.
(58) Novikovskii, A. A.; Gunchenko, P. A.; Prikhodchenko, P. G.; Serguchev, Y. A.; Schreiner, P. R.; Fokin, A. A. *Russ. J. Org. Chem.* **2011**, *47*, 1293−1299.
(59) Fokin, A. A.; Chernish, L. V.; Gunchenko, P. A.; Tikhonchuk, E. Y.; Hausmann, H.; Serafin, M.; Dahl, J. E. P.; Carlson, R. M. K.; Schreiner, P. R. *J. Am. Chem. Soc.* **2012**, *134*, 13641−13650.
(60) Waske, P. A.; Meyerbroker, N.; Eck, W.; Zharnikov, M. *J. Phys. Chem. C* **2012**, *116*, 13559−13568.
(61) Dewar, M. J. S. *J. Am. Chem. Soc.* **1984**, *106*, 669−682.
(62) Brown, R. S.; Nagorski, R. W.; Bennet, A. J.; McClung, R. E. D.; Aarts, G. H. M.; Klobukowski, M.; McDonald, R.; Santarsiero, B. D. *J. Am. Chem. Soc.* **1994**, *116*, 2448−2456.
(63) Meijer, E. W.; Kellogg, R. M.; Wynberg, H. *J. Org. Chem.* **1982**, *47*, 2005−2009.
(64) Tabushi, I.; Aoyama, Y.; Takahash, N.; Gund, T. M.; Schleyer, P. V. R. *Tetrahedron Lett.* **1973**, 107−110.
(65) Schreiner, P. R.; Lauenstein, O.; Butova, E. D.; Gunchenko, P. A.; Kolomitsin, I. V.; Wittkopp, A.; Feder, G.; Fokin, A. A. *Chem.—Eur. J.* **2001**, *7*, 4996−5003.
(66) Deshayes, S.; Liagre, M.; Loupy, A.; Luche, J. L.; Petit, A. *Tetrahedron* **1999**, *55*, 10851−10870.
(67) Schreiner, P. R.; Fokina, N. A.; Tkachenko, B. A.; Hausmann, H.; Serafin, M.; Dahl, J. E. P.; Liu, S. G.; Carlson, R. M. K.; Fokin, A. A. *J. Org. Chem.* **2006**, *71*, 6709−6720.
(68) Roth, S.; Leuenberger, D.; Osterwalder, J.; Dahl, J. E.; Carlson, R. M. K.; Tkachenko, B. A.; Fokin, A. A.; Schreiner, P. R.; Hengsberger, M. *Chem. Phys. Lett.* **2010**, *495*, 102−108.
(69) (a) Frisch, M. J.; Trucks, G. W.; Schlegel, H. B.; Scuseria, G. E.; Robb, M. A.; Cheeseman, J. R.; Scalmani, G.; Barone, V.; Mennucci, B.; Petersson, G. A.; Nakatsuji, H.; Caricato, M.; Li, X.; Hratchian, H. P.; Izmaylov, A. F.; Bloino, J.; Zheng, G.; Sonnenberg, J. L.; Hada, M.; Ehara, M.; Toyota, K.; Fukuda, R.; Hasegawa, J.; Ishida, M.; Nakajima, T.; Honda, Y.; Kitao, O.; Nakai, H.; Vreven, T.; J. A. Montgomery, J.Peralta, J. E.; Ogliaro, F.; Bearpark, M.; Heyd, J. J.; Brothers, E.; Kudin, K. N.; Staroverov, V. N.; Kobayashi, R.; Normand, J.; Raghavachari, K.; Rendell, A.; Burant, J. C.; Iyengar, S. S.; Tomasi, J.; Cossi, M.; Rega, N.; Millam, J. M.; Klene, M.; Knox, J. E.; Cross, J. B.; Bakken, V.; Adamo, C.; Jaramillo, J.; Gomperts, R.; Stratmann, R. E.; Yazyev, O.; Austin, A. J.; Cammi, R.; Pomelli, C.; Ochterski, J. W.; Martin, R. L.; Morokuma, K.; Zakrzewski, V. G.; Voth, G. A.; Salvador, P.; Dannenberg, J. J.; Dapprich, S.; Daniels, A. D.; Farkas, O.; Foresman, J. B.; Ortiz, J. V.; Cioslowski, J.; Fox, D. J., *Gaussian 09*, Revision D.01, Gaussian, Inc.: Wallingford CT, 2009. (b) Johnson, E. R.; Keinan, S.; Chaudret, R.; Piquemal, J.-P.; Beratan, D. N.; Yang, W. *J. Chem. Theory Comput.* **2011**, *7*, 625−632. (c) Johnson, E. R.; Keinan, S.; Mori-Sanchez, P.; Contreras-Garcia, J.; Cohen, A. J.; Yang, W. *J. Am. Chem. Soc.* **2010**, *132*, 6498−6506.
(70) Courtney, T.; Johnston, D. E.; Rooney, J. J.; McKervey, M. A. *J. Chem. Soc., Perkin Trans. 1* **1972**, 2691−2696.

DOI: 10.1021/jacs.5b01555
J. Am. Chem. Soc. 2015, 137, 6577−6586